ACS chemical biology

Articles

pubs.acs.org/acschemicalbiology

Noncompetitive Modulation of the Proteasome by Imidazoline Scaffolds Overcomes Bortezomib Resistance and Delays MM Tumor Growth *in Vivo*

Theresa A. Lansdell,[†] Michelle A. Hurchla,[‡] Jingyu Xiang,[‡] Stacy Hovde,[§] Katherine N. Weilbaecher,[‡] R. William Henry,[§] and Jetze J. Tepe*[,†]

Departments of [†]Chemistry and [§]Biochemistry & Molecular Biology, Michigan State University, East Lansing, Michigan, United States

[‡]Department of Medicine, Division of Oncology, Washington University School of Medicine, St. Louis, Missouri, United States

Supporting Information

ABSTRACT: Multiple myeloma (MM) is a malignant disorder of differentiated B-cells for which standard care involves the inhibition of the proteasome. All clinically used proteasome inhibitors, including the chemotherapeutic drug bortezomib, target the catalytic active sites of the proteasome and inhibit protein proteolysis by competing with substrate binding. However, nearly all (~97%) patients become intolerant or resistant to treatments within a few years, after which the average survival time is less than 1 year. We describe herein the inhibition of the human proteasome *via* a noncompetitive mechanism by the imidazoline scaffold, TCH-13. Consistent with a mechanism distinct from that of competitive inhibitors, TCH-013 acts additively with and overcomes resistance to bortezomib. Importantly, TCH-013 induces apoptosis in a panel of myeloma and leukemia cell lines, but in contrast, normal lymphocytes, primary bone marrow stromal cells (hBMSC), and macrophages are resistant to its cytotoxic effects. TCH-013 was equally effective in blocking MM cell growth in co-cultures of MM cells with hBMSC isolated from CD138 negative bone marrow (BM) samples of MM patients. The cellular activity translated well *in vivo* where TCH-013 delayed tumor growth in an MM xenograft model to a similar extent as bortezomib.

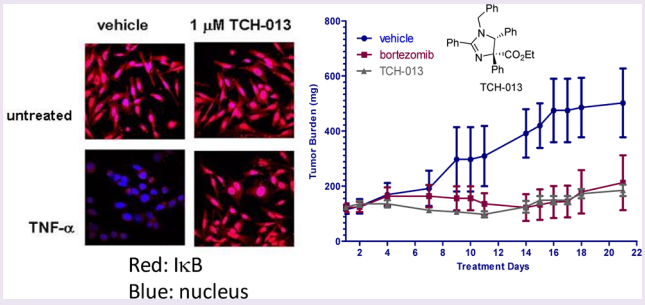

Multiple myeloma (MM) is a malignant disorder of differentiated B-cells that remains largely incurable, with nearly all patients relapsing.[1] MM cells are predominantly located in the bone marrow where they closely interact with bone marrow stromal cells (BMSCs).[2] MM cell growth, survival, migration, and drug resistance is dictated by the tumor microenvironment through direct cell-to-cell contact or indirectly *via* secretion of cytokines and soluble growth factors, such as interleukin 6 (IL-6), VEGF, TNF-α, and others.[3−5] Of these cytokines, IL-6 plays a predominant role in the terminal differentiation of B cells and is critical in the pathogenesis of MM.[2,6] The interactions between MM cells and BMSCs augments IL-6 secretion *via* the nuclear factor-κB (NF-κB) pathway, resulting in increased proliferation and inhibition of apoptosis of MM cells.[6−8] In addition to BMSCs, osteoclasts also strongly enhance contact-mediated growth and survival of MM cells. Thus, the microenvironment of the bone marrow plays an integral role in the pathogenesis of MM, stimulating a vicious cycle of cytokine production, tumor growth, and bone destruction.[9,10] Disruption of this cycle by therapeutics is accomplished by inhibition of the proteasome, which has subsequently evolved to become the central standard of care for MM treatment.[11−13]

The 26S proteasome consists of a 20S catalytic core and 19S regulatory particles.[14−16] The 19S regulatory particles are responsible for recognition, unfolding, and translocation of substrates into the 20S core.[17] The 20S catalytic core is a threonine protease that exhibits three distinct proteolytic activities: chymotrypsin-like (CT-L), trypsin-like (T-L), and caspase-like (Casp-L) activity, which are responsible for proteolytic degradation of its substrates.[18] All clinically relevant proteasome inhibitors, including the peptide-based drug bortezomib (Figure 1A), elicit their activity *via* the same mechanism: formation of a covalent bond to the ^{1}N terminal threonine in the catalytic sites of the enzyme.[11,19−22] These competitive inhibitors directly compete with substrate binding to the active site(s) in the proteasome. At the cellular level, drug resistance has been attributed, in part, to overexpression of a mutated form of the catalytic subdomains, abrogating drug−protein binding.[23−26] However, tumors that exhibit resistance *via* this mechanism will retain sensitivity to drugs that bind outside the active site inhibiting activity of the enzyme *via* a

Received: October 20, 2012
Accepted: November 30, 2012
Published: November 30, 2012

   dx.doi.org/10.1021/cb300568r | *ACS Chem. Biol.* 2013, 8, 578−587

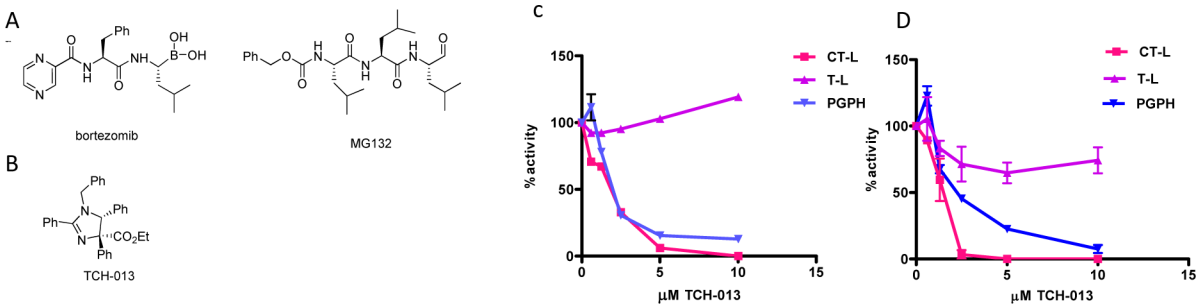

Figure 1. (A) Chemical structures of peptide-based competitive inhibitors bortezomib and MG132 and (B) noncompetitive proteasome, small molecule inhibitor TCH-013. (C) TCH-013 inhibits the CT-L and Casp-L activity of the human proteasome. Fluorogenic substrates Suc-LLVY-AMC, Z-ARR-AMC, and Z-LLE-AMC were used to measure CT-L, T-L, and Casp-L activities of purified human 20S proteasome particles as described in Methods. The maximum increase in fluorescence per minute was used to calculate specific activities of each sample. (D) Fluorogenic substrates Suc-LLVY-AMC. Z-ARR-AMC and Z-LLE-AMC were used to measure CT-L, T-L, and Casp-L activities of fully assembled proteasomes extracted from RPMI-8226 human multiple myeloma cells with ATP/DTT buffer as described in Methods. The maximum increase in fluorescence per minute was used to calculate specific activities of each sample.

noncompetitive mechanism.[27−31] Aside from overcoming resistance,[32] it has also been suggested that noncompetitive modulation of enzyme activity limits off-target effects, reducing toxicity.[28,31,33] Unfortunately, examples of noncompetitive proteasome inhibitors are very rare. PR-39, a 39-amino-acid peptide, inhibits the 20S proteasome noncompetitively *via* this type of allosteric mechanism, where binding to the α-ring of the 20S proteasome leads to changes in proteasome structure and prevents degradation of specific substrates, including IκB.[34−36] As for small molecule inhibitors, chloroquine binds to a region of the α-ring but only at lethal, nonphysiologically relevant concentrations (>40 μM).[37] Schimmer and co-workers reported that 5AHQ inhibits the proteasome through a noncompetitive mechanism; however, it is unclear if this is *via* a direct proteasome-drug interaction or upstream event.[32] In addition, the nonpromiscuous secondary fungal metabolite gliotoxin has also been shown to bind *via* disulfide bonds to the proteasome but exhibits a multitude of cellular effects and high general toxicity.[38]

Although bortezomib is undoubtedly one of the biggest breakthroughs in this field, additional treatment options are necessary as nearly all (~97%) patients become intolerant or resistant to these competitive inhibitors within a few years, after which the average survival time is less than one year.[39] We have previously reported that nonpeptide based, trans-imidazoline TCH-013 (Figure 1B) and its *R,R* enantiomer TCH-013a are orally available antiarthritic agents that modulate NF-κB-mediated cytokine production *via* an unknown mechanism.[40,41] Considering the important role of cytokine production in the pathogenesis of MM, we subsequently evaluated these agents for their mechanistic details and potential efficacy for MM treatment. Herein, we report that the mechanism of NF-κB-mediated cytokine inhibition by TCH-013 proceeds *via* a noncompetitive modulation of the proteasome. We show that TCH-013 binds to a site distinct from the substrate binding sites and overcomes resistance to competitive proteasome inhibitors. TCH-013 induces apoptosis in a panel of myeloma and leukemia cell lines. In contrast, normal lymphocytes, primary bone marrow stromal cells, and macrophages were resistant to the cytotoxic effects. MM−bone marrow stromal cell co-culture systems indicate that the efficacy of TCH-013 to induce MM cell death is not affected by bone marrow microenvironment. Finally, we show that TCH-013 prevents tumor growth in an MM xenograft mouse model to a similar extent as the maximum tolerated dose of bortezomib.

RESULTS AND DISCUSSION

TCH-013 Inhibits the Catalytic Activity of the Proteasome As Measured *in Vitro* in Purified 20S Proteasome and in Cell Culture. Previously, our lab demonstrated that TCH-013 inhibits the activation of NF-κB mediated IL-6 transcription through an unknown mechanism.[41] NF-κB activation is tightly controlled by its inhibitory protein, IκB, which in turn is controlled by the ubiquitin-proteasome system (UPS). Thus, in order to elucidate the mechanism of NF-κB inhibition by TCH-013, the ability of TCH-013 to inhibit the proteasome was investigated *in vitro* and in cell culture. Purified 20S proteasome and the following fluorogenic substrates at their respective K_M values (Supplementary Figure 1) were used: Suc-LLVY-AMC (for CT-L activity), Boc-LRR-AMC (for T-L activity), and Z-LLE-AMC (for Casp-L activity).[30] The rates of hydrolysis were monitored by fluorescence increase over time, and the linear portions of the curves were used to calculate the IC_{50} values (Figure 1C). *In vitro* analysis indicates that TCH-013 selectively inhibits the CT-L, (IC_{50} 2.80 ± 0.66 μM) and Casp-L (IC_{50} 1.60 ± 0.26 μM) activities of the 20S catalytic core of the human proteasome. The T-L activity was not inhibited. Consistent with *in vitro* results, TCH-013 also inhibited the CT-L and Casp-L activity in cell extracts from MM cells RPMI-8226 (Figure 1D), with no significant activity toward the T-L activity. These data indicate that TCH-013 inhibits the 20S proteasome in purified protein assays as well as in crude MM cell extracts at similar efficacies, thus making it unlikely that activity is controlled by an indirect upstream regulation of the proteasome in the cell.

TCH-013 Is Not a Promiscuous Inhibitor and Does Not Form Aggregates or Micelles. In order to examine whether TCH-013 exhibits protease selectivity, we evaluated the compound against various proteases, including the 20S human immunoproteasome, 20S proteasome isolated from *S. cerevisiae* (Supplementary Figure 2), calpain, and trypsin (data not shown). TCH-013 was found to be equally effective in modulating the different types of purified 20S proteasomes but was devoid of any activity against the other proteases tested. These data indicate that TCH-013 selectively inhibits the proteasome over other proteases tested. False positives in *in*

dx.doi.org/10.1021/cb300568r | *ACS Chem. Biol.* 2013, 8, 578−587

vitro assays can often be observed when amphipathic molecules form colloidal aggregates in aqueous buffers.[42] We tested TCH-013 in various assays to examine the possibility of aggregation or micelle formation.[43] TCH-013 did not form micelles or aggregates at relevant concentrations. The various assays and results are described in detail in Supplementary Figure 3 and Supplementary Table 1.

TCH-013 Induces a Modest Accumulation of Ubiquitinylated Proteins in Cell Culture and Prevents the Degradation of IκBα. The 26S proteasome is responsible for the proteolytic degradation of proteins in order to maintain biological homeostasis. Protein ubiquitinylation typically precedes proteasome-mediated proteolytic degradation, and thus inhibition of the proteasome results in an accumulation of ubiquitinylated cellular proteins.[44] To investigate whether TCH-013 inhibits the proteasome in cells, we examined the accumulation of ubiquitinylated cellular proteins. Confocal microscopy was performed on HeLa cells following 2 h of incubation with either vehicle (0.1% DMSO) or TCH-013 (1.0 μM) to detect and localize the accumulation of ubiquitinylated protein (soluble or insoluble) in whole cells. A relatively low dose of TCH-013 was used (1.0 μM) to avoid significant cell death. Treatment of the cells with TCH-013 resulted in an increase in cellular ubiquitin accumulation as measured by anti-ubiquitin immunofluorescence assays (Figure 2A). Quantification of the fluorescent intensity of the ubiquitin−alexa568 conjugates indicated a statistically significant increase (33% fold increase) in accumulation of ubiquitinylated proteins (p = 0.0291), consistent with a mechanism of proteasome inhibition.

One of the many pathways the proteasome regulates is the pro-inflammatory, anti-apoptotic NF-κB signaling pathway, *via* the proteolytic degradation of NF-κB endogenous inhibitor, IκB.[45] In response to cytokine stimulation, IκB undergoes phosphorylation and ubiquitinylation, followed by its subsequent proteasomal degradation, which liberates NF-κB for nuclear translocation and gene transcription.[46] Evaluation of IκB protein levels can thus serve as a specific protein indicator of proteasome activity. Considering the previously reported inhibition of NF-κB by TCH-013,[41,47] we subsequently evaluated the proteolytic degradation of NF-κB's inhibitory protein, IκBα. Total inhibition of cellular protein proteolysis was evaluated by Western blot using whole cell extracts from RPMI-8226 (constitutively active NF-κB) and HeLa cells treated with either the competitive proteasome inhibitors bortezomib or MG-132, and TCH-013. When extracts were probed with a polyclonal antibody directed toward ubiquitin, Western blot analysis indicated strong accumulation of ubiquitin products when treated with the competitive inhibitors bortezomib and MG-132, respectively (Figure 2B and C, lane 3). Interestingly, compared to bortezomib or MG-132 only modest levels of total ubiquitinylated products were found in the TCH-013-treated whole cell extracts (Figure 2B and C, lane 4). In contrast, when IκBα immunoprecipitates from HeLa cells were probed for ubiquitin accumulation, both MG-132 and TCH-013 treatment prevented IκBα degradation (Figure 2C, lanes 3 and 4, respectively). RPMI-8226 cells that contain constitutively active NF-κB provided similar results when probed for modified forms of IκBα (Figure 2B, lanes 3 and 4, respectively).

In order to further verify the effect of TCH013 on cellular IκB levels, we utilized confocal microscopy to visualize IκBα in the presence and absence of TCH-013 (1 μM) in HeLa cells with and without stimulation with TNFα. Cells were stained for

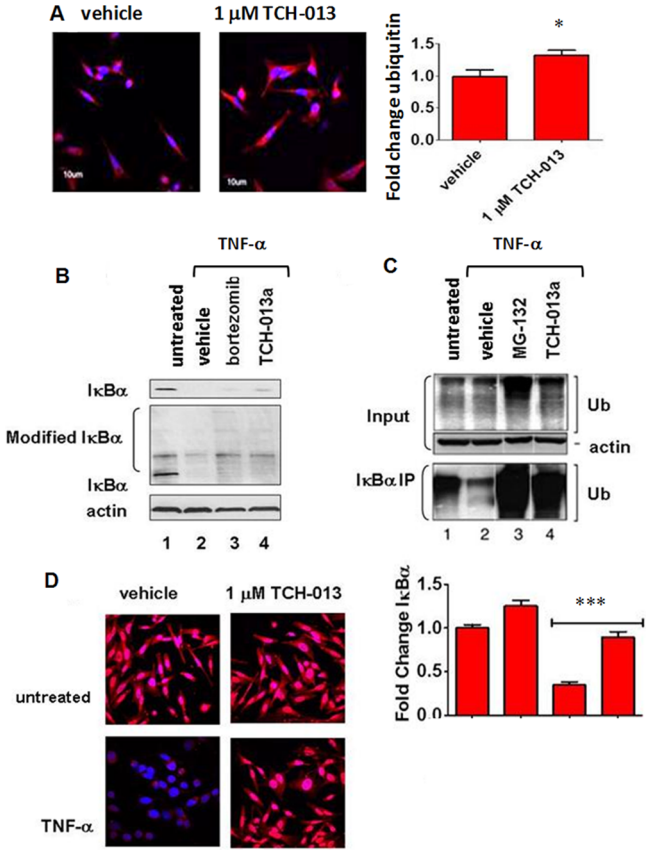

Figure 2. TCH-013 causes the accumulation of ubiquitinylated proteins and inhibits the degradation of IκBα. (A) Representative photos showing fluorescent confocal images of HeLa cells treated with either vehicle or 1 μM TCH-013 for 2 h and subsequently stained for the presence of ubiquitinylated proteins (red) and counterstained for DNA with DAPI (blue). Fluorescent intensity of the ubiquitinylated proteins obtained from each treatment were measured using Olympus FV1000 software (n = 6, p = 0.0291). (B) (top panel) RPMI-8226 cells were left untreated or treated with either vehicle, 1 μM bortezomib, or 10 μM TCH-013 for 30 min and then stimulated with 10 ng/mL TNF-α. Whole cell extracts were probed for the presence of unmodified IκBα using a monoclonal antibody against the N-terminal of IκBα (L35A5). (middle panel) The same whole cell extracts were probed for the presence of unmodified and modified IκBα using a polyclonal antibody against the C-terminal of IκBα (C-21). The presence of actin was used as a loading control on the same blot. (C) HeLa cells were left untreated or treated with either vehicle, 1 μM MG-132, or 10 μM TCH-013 for 30 min and stimulated with 10 ng/mL TNF-α. (input) Whole cell extracts from the samples were probed for the presence of ubiquitin using a monoclonal antibody directed toward ubiquitin (P4D1) that detetects ubiquitin, polyubiquitin, and ubiquitinylated proteins. The presence of actin was used as a loading control. (bottom panel) IκBα was immunoprecipitated from the whole cell extracts using a polyclonal antibody directed toward the C-terminal of IκBα (C-21). The IκBα immunoprecipitates were probed for the presence of ubiquitinylated proteins. (D) Representative photos showing fluorescent confocal images of HeLa cells treated with either vehicle or 1 μM TCH-013 and either stimulated with 10 ng/mL TNF-α or left untreated. The cells were fixed and subsequently stained for the presence of IκBα (red) and counterstained for DNA with DAPI (blue). (n = 6, p = 0.0001).

IκBα with an antibody directed toward the C-terminal of IκBα (red), and DAPI (blue) was used to visualize the DNA. In vehicle-treated cells, IκBα is distributed throughout the cytoplasm of the cells (Figure 2D), whereas upon stimulation

dx.doi.org/10.1021/cb300568r | ACS Chem. Biol. 2013, 8, 578−587

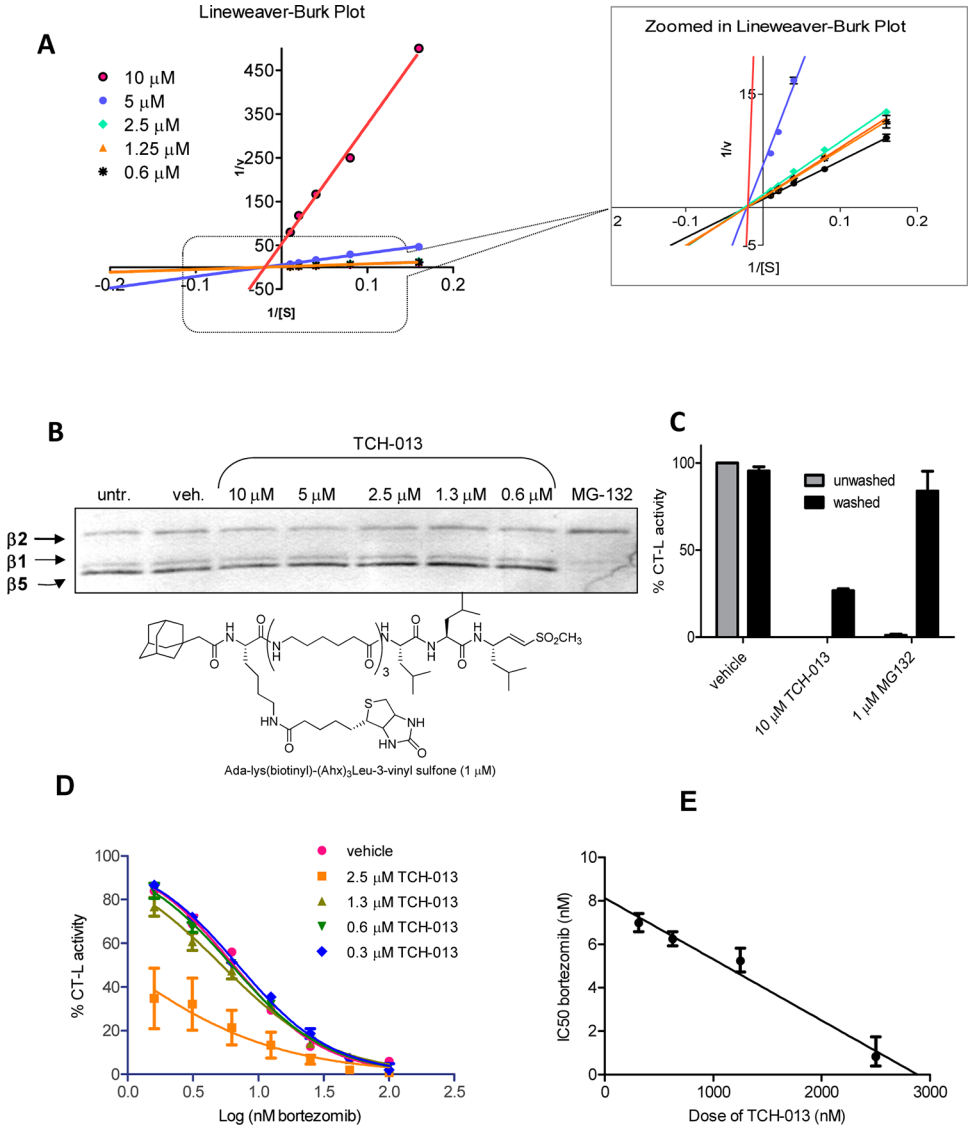

Figure 3. TCH-013 inhibits the 20S proteasome noncompetitively and binds to a site other than the CT-L active site. (A) Kinetic analysis of 20S inhibition by TCH-013 was accomplished using purified human 20S proteasome treated with either: vehicle, 10, 5, 2.5, 1.25, or 0.6 μM TCH-013. K_m and V_{max} values were calculated from Michaelis–Menten analysis using a range of Suc-LLVY-AMC substrate from 1 to 20 μM. (K_m values were 5.35 ± 0.28, 5.40 ± 0.81, 7.37 ± 0.59, 5.66 ± 0.49, 6.02 ± 0.36, and 5.43 ± 0.52 for vehicle, 10, 5, 2.5, 1.25, and 0.6 μM treatment, respectively, while V_{max} values were 0.99 ± 0.03, 0.02 ± 0.001, 0.24 ± 0.01, 0.72 ± 0.03, 0.85 ± 0.03, and 0.82 ± 0.04 U/s for vehicle, 10, 5, 2.5, 1.25, and 0.6 μM treatment respectively). A representative double reciprocal Lineweaver–Burk plot in which all of the treatments result in intersecting on the same point of the *X*-axis (1/[S]) illustrates noncompetitive inhibition. (B) The biotinylated nonreversible covalent and competitive inhibitor Ada-Lys(biotinyl)-$(Ahx)_3$-$(Leu)_3$-vinyl sulfone is not blocked from binding to the catalytic binding sites of the 20S proteasome. Purified human 20S proteasome particles were pretreated for 1 h with vehicle, 10, 5, 2.5, 1.3, or 0.6 μM TCH-013a. Ada-Lys(biotinyl)-$(Ahx)_3$-$(Leu)_3$-vinyl sulfone was then used to probe for catalytic binding sites that were not occupied by TCH-013a. The proteasome particles were then resolved by 12.5% SDS-PAGE and transferred to PVDF. Immunoblotting was performed using an avidin-HRP conjugate. (C) TCH-013 inhibition of the 20S proteasome is not restored after extensive washing. One nanomolar 20S proteasome was treated with vehicle, 10 μM TCH-013 or 1 μM MG-132 and tested for CT-L activity. The treated samples were washed extensively with 500 volumes of assay buffer and tested for CT-L activity. (D) The effect of TCH-013 on CT-L activity of the 20S proteasome is additive to the effect of bortezomib. Dose–response curves of bortezomib in combination with vehicle or varying amounts of TCH-013. (E) TCH-013 and bortezomib retain constant relative potencies as demonstrated by the linear isobole created using the dose of bortezomib necessary to obtain 50% inhibition of CT-L activity with varying amounts of TCH-013.

with TNFα, IκBα is degraded and the fluorescent signal (red) is significantly decreased. Cells treated with TCH-013 prior to TNF-α stimulation retained a robust red fluorescent signal, clearly indicating that TCH-013 inhibits the degradation of IκBα. Quantification of the fluorescent signal illustrates that the prevention of IκBα degradation by TCH-013 is statistically significant (p = 0.0001) when compared to its respective TNF-α/vehicle control. This experiment was repeated with an antibody directed toward the N-terminal of IκBα, which recognizes endogenous levels of total IκBα with similar results (Supplementary Figure 4). These studies indicate that TCH-013 induces the robust accumulation of ubiquitinylated isoforms of IκB, consistent with inhibition of the proteasome.

TCH-013 Inhibits the 20S Proteasome *via* a Non-competitive Mechanism of Binding. Intrigued by the modest accumulation of globally ubiquitinylated proteins, but

dx.doi.org/10.1021/cb300568r | *ACS Chem. Biol.* 2013, 8, 578–587

A

Drug	Cell Line	GI_{50}	Resistance Factor
bortezomib	THP-1	8.1 nM	1.0
	THP-1/BTZ50	386 nM	48.0
	THP-1/BTZ200	759 nM	94.0
	THP-1/BTZ500	2.1 μM	247.0
TCH-013	THP-1	7.3 μM	1.0
	THP-1/BTZ50	8.6 μM	1.2
	THP-1/BTZ200	7.0 μM	0.9
	THP-1/BTZ500	6.8 μM	0.9

B

Cell line	GI_{50} (μM)
MM and Leukemia Cells	
CCRF-CEM	2.79
K562	3.14
MOLT4	3.55
SR	3.24
RPMI-8226	1.84
Normal Cells	
Bone Marrow Macrophages	14.05
Bone Marrow Stromal Cells	>20

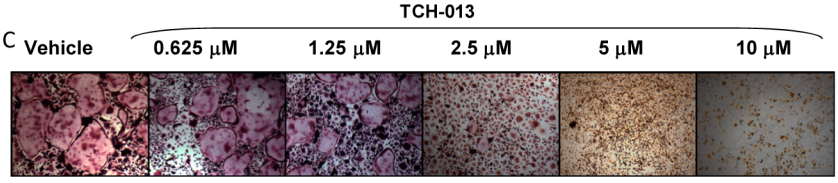

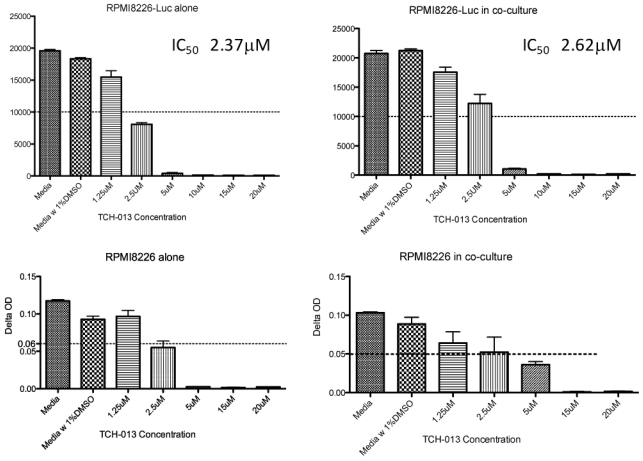

Figure 4. (A) TCH-013 inhibits cell growth in bortezomib (BTZ)-resistant THP-1 cells that overexpress mutated β5 subunits. Parental and BTZ-resistant THP-1 cell lines were treated with TCH-013 continuously for 72 h, and viability was measured using a MTS dye conversion assay. Resistance factor is an expression of the GI_{50} of the BTZ-resistant THP-1 cell line divided by the CC_{50} of the parental THP-1 cell line. (B) *In vitro* viability testing results for leukemia, myeloma, and supportive primary cell lines. (C) Murine bone marrow derived macrophages (mononuclear cells) were cultured under osteogenic differentiation conditions (50 ng/mL M-CSF and 50 ng/mL RANKL) in the continual presence of vehicle or indicated concentrations of TCH-013. Formation of multinucleated osteoclasts is visualized by tartrate-resistant acid phosphatase (TRAP) staining on day 6. At concentrations similar to those required to exert tumor cells cytotoxicity, TCH-013 inhibited the formation of multinucleated osteoclasts. (D) Survival of RPMI8226 cells alone (left) or in the presence of human BMSCs (right) as measured by luciferase activity (top panels) and MTT Assay (bottom panels). Cells were incubated with various concentrations of TCH-013 ranging from 1.25 to 20 μM. The IC_{50} was determined by Prism (Graphpad).

robust accumulation of IκBα in both cell types, we examined in detail the mechanism for proteasome inhibition by TCH-013. For these studies we used the *R,R*-enantiomer, TCH-013a, to ensure clear kinetic results. The mechanism by which TCH-013a inhibits the proteasome was investigated using Michaelis–Menten analysis to determine of K_M and V_{max} and then further illustrated using a Lineweaver–Burk double reciprocal plot of the kinetic data. Kinetic analysis of CT-L activity of purified 20S particles indicated that when the substrate (Suc-LLVY-AMC) concentration was increased incrementally and measurements were taken at five different concentrations of TCH-013a or vehicle, the V_{max} of the CT-L activity diminished with the increasing concentration of substrate and the K_M remained constant (Figure 3A). This is a pattern that is consistent with a noncompetitive type of inhibition.[48] By contrast, the proteasome inhibitor MG-132 (Figure 1A), which binds the active site of the proteasome, inhibits the human 20S proteasome *via* a competitive-type mechanism (data not shown). The results suggest that the site(s) of TCH-013 binding on the 20S proteasome is not directly in competition with substrate binding and proceeds *via* a noncompetitive mechanism of binding. The K_i values (2.4 μM ± 0.4) were determined using a Dixon plot (Supplementary Figure S5) and matched the IC_{50} value (IC_{50} 2.80 ± 0.66 μM), which is also consistent with noncompetitive kinetics.

TCH-013 Binds to a Site(s) Other than the Catalytic Site. Noncompetitive binding kinetics implies that an inhibitor binds to a site on the enzyme that is distinct from the substrate binding site. We examined if TCH-013a binds to a site other than the substrate binding site using a probe directed toward the catalytic subunits of the 20S proteasome (Figure 3B). Purified 20S enzyme was pretreated for 1 h with vehicle, an excess of MG-132 (1 μM), or an excess of TCH-013a (10 μM). The drug-bound enzyme was then probed with 1 μM biotinylated adamantane-acetyl-(6-aminohexanoyl)$_3$(leucinyl)-3-vinyl-(methyl)-sulfone (a potent, covalent, irreversible inhibitor of all three catalytic subunits) at an amount determined to give 50% the maximum binding to the catalytic center of the β5 subunit (Supplementary Figure 6).[49] The samples were electrophoresed, transferred to PVDF, and probed for the biotin label. The results shown in Figure 3 indicate that treatment of the 20S proteasome with MG-132 blocked the binding of the biotinylated probe to the β5 catalytic binding site.[49] However, pretreatment of the enzyme for 1 h with TCH-013a at concentrations ranging from 0.6 to 10 μM had no effect on the binding of the probe to any of the catalytic sites (β5, β1, or β2).

A difference in binding affinity between TCH-013a and the biotinylated probe for the active sites of the 20S proteasome could allow the probe to compete with TCH-013a and bind to the catalytic subunits as seen in Figure 3B. On the basis of the

dx.doi.org/10.1021/cb300568r | *ACS Chem. Biol.* 2013, 8, 578–587

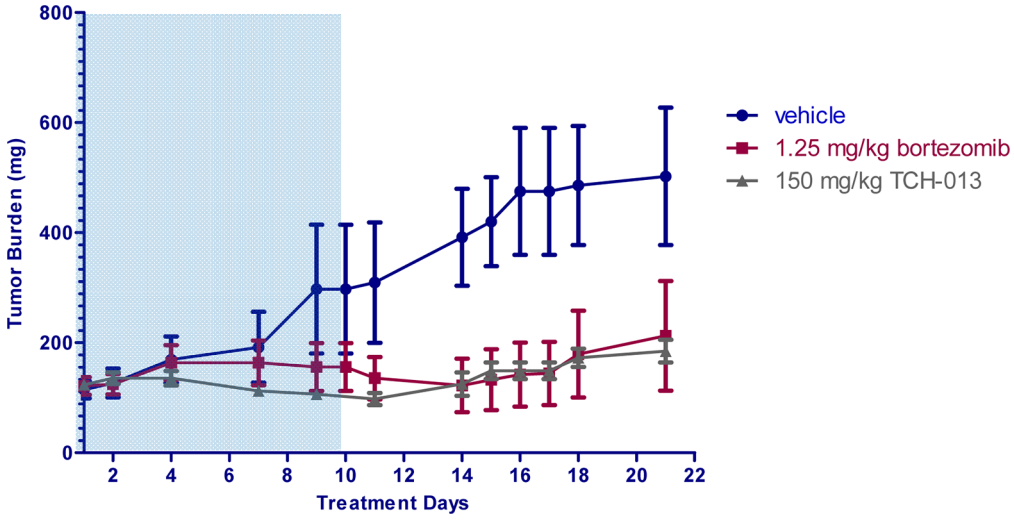

Figure 5. TCH-013 delays tumor growth in a RPMI-8226 xenograft mouse model. The antitumor activity of TCH-013 against established RPMI-8226 human MM in female NIH-III mice was evaluated as described in Methods. TCH-013 was administered IP at 150 mg/kg twice daily. Bortezomib was administered intravenously twice weekly at the maximum tolerated dose. Tumor burden (mg) = $(L \times W^2)/2$, where L and W are the respective orthogonal tumor length and width measurements (mm). Shaded area included treatment days.

noncompetitive kinetics of TCH-013a this would seem unlikely. However, we further challenged this possibility by evaluating the reversibility of TCH-013a binding to the enzyme, compared to MG-132, using membrane washout experiments. Treatment of the 20S proteasome with TCH-013a or MG-132 completely abrogated the CT-L activity of the enzyme. After extensively washing with 500 volumes of activity buffer on a membrane concentrator, the retentates were analyzed again for 20S CT-L activity (Figure 3C). Removal of MG-132 by extensive washing with reaction buffer completely restored proteolytic activity. Unlike the reversible competitive inhibitor MG-132, the proteolytic activity of the 20S proteasome was not restored for TCH013a-treated samples (Figure 3C, >70% inactive), indicating that either TCH-013a is strongly bound to the enzyme or that the enzymatic activity is irreversibly compromised. Thus, consistent with our kinetic results, the catalytic sites are free to bind with the biotinylated probe in the presences of proteasome-bound TCH-013a.

Given that TCH-013 inhibits the proteasome at a site that is distinct from competitive inhibitors such as bortezomib, we determined the effect of the combination of TCH-013 and bortezomib on the CT-L activity of the proteasome. When added to the proteasome in combination, both TCH-013 and bortezomib retained a linear relationship of relative potencies indicating that the agents act additively when added in combination to the 20S proteasome (Figure 3D and E) in the purified enzyme assay. This additive effect translated in cell culture where the combination treatment of bortezomib and TCH-013 in multiple myeloma cells indicated additive effects of the compounds (Supplementary Figure 7). These data further support our findings that both agents affect proteasome activity *via* distinct mechanisms.

TCH-013 Induces Rapid Cell Death in Bortezomib-Resistant THP-1 Cells. Although recent advances in the treatment of MM have made a dramatic impact, nearly all patients relapse.[50] Several mechanisms of resistance have been identified, including mutation and overexpression of the β5 catalytic subunit of the proteasome.[24] Inhibitors with mechanisms that are distinct from these competitive inhibitors, such as bortezomib (BTZ), could bypass this type of resistance. Given that TCH-013 binds to a site(s) other than the substrate binding sites of the proteasome, we evaluated the cytotoxicity of TCH-013 in bortezomib-resistant human myelomonocytic THP-1 cells. The mechanism of acquired resistance in this cell line was previously determined to be due to the overexpression of a mutated β5 catalytic subunit of the proteasome. Proteasomes assembled with this mutant subunit also exhibited strong cross-resistances across the board of competitive proteasome inhibitors.[24] Wild-type THP-1 and THP-1 cells with increasing levels of bortezomib resistance (THP-1/BTZ50, THP-1/BTZ200 and THP-1/BTZ500 cells) were treated with TCH-013 or bortezomib (control), and cell viability was measured after 72 h using an MTS assay (Figure 4A). THP-1/BTZ50, THP-1/BTZ200, and THP-1/BTZ500 were 48-, 94-, and 247-fold [24] more resistant to bortezomib, respectively. Importantly, TCH-013 retained efficacy against the bortezomib-resistant cell lines and displayed similar potency regardless of the extent of bortezomib resistance. These results are consistent with the observed drug−proteasome binding interaction that is distinct from the binding of competitive type inhibitors, such as bortezomib.

TCH-013 Induces Cell Death in MM Cells. In order to assess whether noncompetitive proteasome inhibition effectively kills MM cells, the cytotoxicity of TCH-013 was evaluated on a panel of myeloma and leukemia cell lines, as well as supportive bone marrow stromal cells, macrophages, and osteoclasts in cell culture. As indicated in Figure 4B, TCH-013 significantly decreased viability of myeloma and leukemia cell lines (GI_{50} 1−4 μM). In contrast, primary bone marrow stromal cells, and macrophages were resistant to the cytotoxic effects of TCH-013 with GI_{50}'s of 14 to >20 μM (Figure 4B). Notably, these levels exceed the maximum serum concentration of TCH-013 that is attained following intraperitoneal injections (Supplementary Figure 8).

In addition to its antitumor properties, an important mechanism of bortezomib is its ability to prevent pathological bone resorption by inhibiting osteoclast differentiation and resorption.[51] Similar to these positive side effects of bortezomib, treatment of bone marrow macrophages with TCH-013 inhibited their differentiation into multinucleated,

dx.doi.org/10.1021/cb300568r | *ACS Chem. Biol.* 2013, 8, 578−587

bone-resorbing osteoclasts at concentrations similar to those required to induce cytotoxicity in tumor cells (Figure 4C).

The supporting microenvironment of the BMSC induces MM survival and renders many therapeutic options less effective. Given the notable lack of toxicity to the primary bone marrow stromal cells but excellent cytotoxicity to the MM cells, we investigated the efficacy of TCH-013 in co-cultures of MM cells with hBMSC isolated from CD138-negative BM samples of MM patients, as a model for this natural microenvironment. In order to differentiate the MM cells from primary hBMSC, we used RPMI-8226-luc cells in order to visualize cytotoxicity of MM cells by a decrease in luciferase activity. We found that TCH-013 induced cell death in both isolated MM cells and in MM cells co-cultured with hBMSC (Figure 4D). The reduction of luciferase activity, indicative of survival of the RPMI-8226-luc cells for both MM alone (IC_{50} 2.37 μM) and co-cultured (IC_{50} 2.62 μM), is inconsistent with our previous cytotoxity data in isolated MM cells (GI_{50} 1.84 μM).

To further examine the time course for apoptosis induced by bortezomib and TCH-013, RPMI-8226 cells were incubated with these compounds, and the percentage of cells exhibiting an apoptotic phenotype was determined by propidium iodide staining and fluorescence activated cell sorting (FACS) to measure cellular chromosomal DNA content (Supplementary Figure 8A). The DNA content per cell can be used as a diagnostic indicator of cells in the G1 (2N content), G2 (4N content), and S (between 2N and 4N content) phases. The labeling of cells with apparent DNA content less than the G1 peak (sub-G1) demonstrates that DNA fragmentation has occurred and is suggestive of apoptosis. TCH-013 (at 5× GI_{50}, 10 μM) induced DNA fragmentation rapidly, indicative of programmed cell death or apoptosis, with a similar percentage of cells exhibiting a sub-G1 staining pattern over time, as compared to the clinically used MM drug bortezomib (at 500× $GI_{50,}$ 1.0 μM) (Supplementary Figure 8B). These data indicate that TCH-013 can induce substantial and rapid apoptosis in MM cells.

TCH-013 Is Well Tolerated in Nontumor Bearing Immunocompetent Mice and Effective in a RPMI-8226 Mouse Xenograft Model. In order to evaluate whether tumoral cytotoxicity translates *in vivo*, we determined the activity of TCH-013 against established RPMI-8226 human MM in female NIH-III mice (Figure 5). The study, using four to six mice per group, evaluated the efficacy of 150 mg/kg TCH-013 administered intraperitoneal on tumor cell growth and host survival. This dose was determined to obtain serum levels of about 5 μM 3 h post IP injection with a half-life of 3.3 h (Supplementary Figure 9). The study had a control cohort treated with the vehicle alone (10% propylene glycol in sterile water). The mice were inoculated subcutaneously, high in the right axilla with RPMI-8226 MM cells with 76.4% of the animals developing measurable tumors. Treatment began when the mean estimated tumor mass for all groups was 122 mg (range, 111−124 mg). Mice were then assigned to treatment groups (0.2 mL/20g 10% propylene glycol in sterile water twice a day for 8 days then 2 days off, 1.25 mg/kg bortezomib intravenously once a day for 3 days then 2 days off, and 150 mg/kg TCH-013 twice a day for 8days then 2 days off). This dosing regimen did not indicate any detectable anemia, gross neurologic toxicity (data not shown), weight loss, or liver toxicity as earlier reported.[40] In a log−linear regression model of the mice during treatment (Supplementary Figure 10), the mean tumor volume doubling time was 6.3 days for the vehicle-treated group and >25 days for TCH-013 ($P < 0.0001$). Of the bortezomib-treated mice, 50% exhibited no tumor growth during the treatment period, and 17% of the bortezomib-treated mice experienced complete tumor regression after treatment was removed. The remainder of the bortezomib-treated mice had a mean tumor doubling time of 20 days. Fifty percent of the TCH-013-treated mice also did not exhibit tumor growth during the treatment period. The other half of the TCH-013-treated mice had a doubling time longer than 25 days ($n = 4$, $P < 0.0001$ when compared to the vehicle treated group) during the 10 day treatment period. Tumors began to grow after the cease of treatment on day 10 for both the bortezomib- and TCH-013-treated groups, at similar doubling rates.

Conclusion. Without doubt, competitive proteasome inhibitors significantly improve the clinical outcome of patients with MM; however, inherent toxicity (*e.g.*, neuropathy and cytopenias) and cross-resistance is often observed in patients undergoing treatment. Nearly all patients eventually become resistant and/or intolerant, after which the survival average is less than 1 year.[12,13,39] Resistance to bortezomib has been demonstrated to occur through several different mechanisms, including the overexpression of mutated catalytic subunits of the proteasome,[24,25] which is the site in the proteasome where bortezomib and all other proteasome inhibitors under clinical evaluation bind.[11] In this study, we examined TCH-013, a non-peptide-based, small molecule NF-κB inhibitor.[40,41] Michaelis−Menten kinetics demonstrates that TCH-013 inhibits the CT-L and Casp-L activities of the 20S proteasome *via* non-competitively kinetics. Our data verifies that TCH-013 binds to site(s) other than the substrate binding site consistent with a mechanism distinct from competitive proteasome inhibitors. Importantly, TCH-013 acted additively with and overcame resistance to the competitive proteasome inhibitor bortezomib, consistent with a mode of action distinct from competitive proteasome inhibitors.

In addition, TCH-013 induced cell death in myeloma and leukemia cells preferentially over normal hematopoietic and stromal cells and indicated activity in MM cells co-cultured with primary human BMSC isolated from CD138-negative BM samples of MM patients. Similar to bortezomib, TCH-013 was found to be effective as a single agent in MM cells albeit at higher concentrations than bortezomib. However, the GI_{50} of TCH-013 in the RPMI-8226 MM cell lines was comparable to the clinically significant drugs doxorubicin but better than melphalan.[13] The concentration at which TCH-013 induced cell death in myeloma cells was similar to concentrations at which it inhibited the proteasome and blocked NF-κB transcription, which suggests that the cytotoxicity of TCH-013 is related to its effects on protein degradation by the proteasome. The efficacy of TCH-013 on RPMI-8226 cells in cell culture translated well into the RPMI-8226 mouse xenograft model. Mice treated with TCH-013 (150 mg/kg) resulted in a significant delay in tumor growth during the treatment period. This markedly delayed tumor growth was comparable to bortezomib treatment at its maximum tolerated dose. These studies indicate that the noncompetitive inhibitor TCH-013 was effective in blocking MM tumor growth *in vivo*.

The binding site(s) at which TCH-013 noncompetitively inhibits the proteasome is not known at this time, and examples of noncompetitive proteasome modulators are scarce. One possibility is that TCH-013 binding induces a conformational

change that prevents certain substrates from entering the proteolytic chamber of the proteasome complex. Detailed co-crystal structures of the TCH-013−proteasome interaction may reveal the binding site(s) by which noncompetitive inhibitors interact with the proteasome.

In conclusion, the orally available, well tolerated, *trans*-imidazoline TCH-013 represents a novel class of non-competitive proteasome inhibitor with significant efficacy in the delay of MM tumor growth in mice. Importantly, TCH-013 acts additively with and overcomes resistance to the competitive proteasome inhibitor bortezomib, consistent with a mode of action distinct from competitive proteasome inhibitors.

METHODS

Reagents. Ada-Lys(biotinyl)-(Ahx)3-(Leu)3-vinyl sulfone was purchased from Enzo Life Sciences. Bortezomib was purchased from Selleck Biochemicals, and MG-132 was purchased from EMD. Fluorogenic substrates and purified proteasome particles were purchased from Boston Biochem. All antibodies were purchased from Santa Cruz Biotechnologies and Cell Signaling. Propidium iodide, RNase, and all cell culture media and supplements were purchased from Invitrogen. Luciferase Assay System was purchased from Promega. Black 96-well plates were purchased from Corning, and 1-(4,5-dimethylthiazol-2-yl)-3,5-diphenylformaza (MTT) was purchased from Sigma. All other chemicals were purchased from Sigma.

Cell Culture. The human cell lines HeLa and RPMI-8226 were purchased from American Type Culture Collection. THP1, THP1/BTZ50, THP1/BTZ200, and THP1/BTZ500 were a kind gift from Drs. J. Cloos and G. Jansen, Dept. of Hematology, Research Coordinator Pediatric Oncology/Hematology VU University Medical Center, Cancer Center Amsterdam, Amsterdam, The Netherlands.[24] The hematopoietic cell lines were maintained in RPMI-1640 supplemented with 10% fetal bovine serum, 100 U/mL penicillin, 100 mg/mL streptomycin, 1 mM sodium pyruvate, and 0.2 mM L-glutamine. HeLa cells were maintained in Dulbecco's modified Eagle's medium (DMEM) supplemented with 10% fetal bovine serum, 100 U/mL penicillin, 100 mg/mL streptomycin, 1 mM sodium pyruvate, and 0.2 mM L-glutamine. Cells were cultured at 37 °C, 5% CO_2. hBMSC was isolated from CD138-negative BM samples of MM patients and cultured in MEM Alpha medium with 20% FBS in a cell culture coated plate for about 14−21days (varied between patients), with the medium changed when needed.

Cell Viability Assays. Human white blood cells were counted manually using a BD Unopette reservoir and a hemacytometer. CCRF-CEM, K-562, MOLT-4, RPMI-8226, and SR cell viability was determined in the NCI Developmental Therapeutics Program 60 Cell Line Screen. All other cell line viability was assayed using the MTS dye conversion assay (Promega) in our lab following the manufacturer's protocol. The absorbance of formazan was measured at 490 nm on a SpectraMaxM5e microplate reader. Background absorbance was subtracted from each, measurement, and viability was calculated using the untreated control as 100%. Drug potency was expressed as GI_{50} (concentrations that inhibit viability by 50%). GI_{50} was calculated by a nonlinear regression analysis of the values.

FACS Analysis. Cells were treated with vehicle (0.1% DMSO), bortezomib, or TCH-013 for 0, 8, 16, and 24 h at 37 °C, 5% CO_2. The cells were harvested and resuspended in PBS with 50% FBS. The cells were fixed with 70% ice-cold ethanol overnight. After centrifugation of the cells, the pellet was washed two times with 5 mL ice-cold PBS containing 10% FBS, and resulting the cell pellet was resuspended in staining solutions (PBS containing 50 μg propidium iodide, 10 μL 0.1 M EDTA, 14 units RNaseA). The DNA content was analyzed by flow cytometry using a FACS Vantage SE analyzer with ModFit LT software.

Proteasome Extraction and Measurement of Proteasome Activity. Proteasome was extracted from RPMI-8226 cells with ATP/DTT buffer as previously described by Holyoake.[52] The fluorogenic substrates Suc-LLVY-AMC, Boc-ARR-AMC, and Z-LLE-AMC were used to measure CT-L, T-L, and Casp-L proteasome activities using 1 nM purified 20S proteasome or 10 μg ATP/DTT lysate.[53] The rate of cleavage of fluorogenic peptide substrates was determined by monitoring the fluorescence of released aminomethylcoumarin using a SpectraMax M5e multiwell plate reader at an excitation wavelength of 380 nm and emission wavelength of 460 nm. Fluorescence was measured at 37 °C every minute over a 30 min period, and the maximum increase in fluorescence per minute was used to calculate specific activities of each sample. K_M, K_i, and V_{max} values were calculated from Michaelis−Menten analysis using a concentrations range of Suc-LLVY-AMC (1−20 μM) and TCH-013a (0.6−10 μM).

Detection of Biotinylated Ada-Lys(biotinyl)-(Ahx)3-(Leu)3-vinly Sulfone Labeled Proteasome Subunits. Inhibitors were mixed with 200 ng of the human 20S proteasome isolated from human erythrocytes in enzyme assay buffer (50 mM Tris-HCl pH 7.5) for 1 h at 37 °C. Subsequently 100 nM Ada-Lys(biotinyl)-(Ahx)3-(Leu)3-vinly sulfone was added and incubated for 1 h at 37 °C. Reaction mixtures were boiled with Laemmli's buffer containing 2-mercaptoethanol for 3 min and resolved on 12.5% SDS-PAGE. The proteins were transferred to a polyvinylidiene difluoride membrane. Immunoblotting was performed using avidin-HRP conjugate and developed using ECL detection.

Western Blot Analysis of Whole Cell Lysates and Immunoprecipitates. Harvested cells were washed twice with PBS and suspended in ice-cold lysis buffer (20 mM tris-HCl pH 7.5, 150 mM NaCl, 1 mM Na_2EDTA, 1 mM EGTA, 1% Triton X-100, 1 mM PMSF, 2.5 mM sodium pyrophosphate, 1 mM glycerophosphate, 1 mM Na_3VO_4, and 1 mg/mL leupeptin. The suspension was kept on ice for 20 min and centrifuged at 15,000 × *g* for 10 min at 4 °C. The supernatant was recovered as total cell lysate, and 20 μg lysate was separated on a 10% Tris-HCl gel. Immunoblotting was performed using 1:1000 dilution of the indicated antibodies described below. Mouse monoclonal antibodies were used against the N-terminal of IκBα and ubiquitin (from Cell Signaling) and rabbit polyclonal antibody against the C-terminal of IκBα (Santa Cruz Biotechnology). The secondary antibody, HRP conjugated anti-mouse or anti-rabbit IgG antibody, was used at the dilution of 1:3000. For IκBα immunoprecipitation, whole cell lysates were prepared as above. Approximately 1 mg of protein from whole cell lysates was immunoprecipitated using the rabbit polyclonal antibody against the C-terminal of IκBα (Santa Cruz Biotechnology) following standard procedures. One quarter of the immunoprecipitate was separated on a 10% Tris-HCl gel and transferred to PVDF. Immunoblotting was performed using mouse monoclonal antibody against ubiquitin (Cell Signaling).

Detection of Ubiquitin and IκBα by Confocal Microscopy. HeLa cells were grown on glass coverslips and treated with vehicle (0.1% DMSO) or 1.0 μM TCH-013. After pretreatment with compounds, the cells were stimulated with 20 ng/mL TNF-α (30 min for IκBα and 2 h for ubiquitin experiments), while the control cells were left unstimulated. Cells were then fixed with 4% paraformaldehyde in PBS, permeabilized in 0.5% Triton in PBS, and preincubated for 1 h in blocking buffer (5% BSA, 0.05% Tween-20 in PBS). The cells were stained overnight with primary antibody at 4 °C (1:250 of either rabbit anti-ubiquitin (P4D1), mouse anti-IκBα (L35A5), or rabbit anti-IκBα (C21) in blocking buffer) and for 1 h with Alexa568 labeled secondary antibody (1:1000, Invitrogen). Coverslips were mounted with Fluorogel containing DAPI (4,6-diamidino-2-phenylindole; 1 mg/mL). Cells were imaged using an Olympus FV1000 scanning confocal microscope using the one way XY scan mode.

***In Vitro* Murine Osteoclast Differentiation.** Total bone marrow was isolated from long bones of 8-week old C56Bl/6 mice. Bone marrow derived macrophages (BMM) were generated by culturing first in αMEM supplemented with 100 ng/mL M-CSF for 3 days. To generate mature OCs, BMMs were then replated at 4 × 10^4 cells/mL in αMEM supplemented with 50 ng/mL M-CSF and 50 ng/mL RANKL, refeeding every 48 h for 6 days as previously described.[54]

dx.doi.org/10.1021/cb300568r | *ACS Chem. Biol.* 2013, 8, 578−587

Cells were fixed and stained for TRAP using the leukocyte acid phosphatase kit (Sigma-Aldrich).

MM-hBMSC Co-culture. Human BMSCs were plated in 96-well plates in 20% FBS MEM and allowed to attach for overnight, and then the wells were gently washed with PBS twice. Medium was then exchanged to MEM Alpha with 0.5% FBS, and cells were starved for 12 h. Then medium was exchanged to RPMI-1640 with 0.5% FBS when RPMI-8226-Luc cells were added to the plate with medium alone or in the presence of various concentrations of TCH-013. After 48 h, the survival of the RPMI-8226 cells was assessed by Luciferase Assay System (Promega) per manufacture's instruction and by 1-(4,5-dimethylthiazol-2-yl)-3,5-diphenylformazan (MTT; Sigma) assay.

Human MM Xenograft Model. The RPMI-8226 xenograft model was performed at Charles River Laboratories using Female NIH-III mice (Crl: NIH-Lyst ^{bg}Foxn1^{nu}Btk ^{xid}). Mice were 5−6 weeks old on day 1 of the experiment. A 2.5×10^7 cells/mL suspension (92.35% viable based on trypan blue exclusion) was prepared in 50% serum free media and 50% matrigel. The mice were implanted subcutaneously, high in the right axilla, with 5×10^6 cells in 200 μL using a 27-guage needle attached to a 1 cc syringe. Postinjection viability was determined by trypan blue exclusion to be 76.4%. Tumor burden (mg) was estimated from caliper measurements by the formula for the volume of a prolate ellipsoid assuming unit density as Tumor burden (mg) = $(L \times W^2)/2$, where L and W are the respective orthogonal tumor length and width measurements (mm).

■ ASSOCIATED CONTENT

Supporting Information

This material is available free of charge *via* the Internet at http://pubs.acs.org.

■ AUTHOR INFORMATION

Corresponding Author

*E-mail: tepe@chemistry.msu.edu.

Notes

The authors declare no competing financial interest.

■ ACKNOWLEDGMENTS

The authors gratefully acknowledge financial support in part from the MM Research Foundation (MMRF), the National Institutes of Health (CA-142644-01), Bioscience Research and Commercialization Center (BRCC), and the Michigan Initiative for Innovation & Entrepreneurship (MIIE). The authors would like to thank M. Frame for her technical help with confocal microscopy and C. Geiger and C. Hornick for technical help with the bone marrow studies. We would also like to thank MIR Discovery and Imaging Services/Charles River Laboratories for their work on the RPMI-8226 mouse xenograft model. A great deal of appreciation is given to J. Cloos, G. Jansen, and J. Meerloo for the kind gift of the bortezomib-resistant cell lines.

■ REFERENCES

(1) Mahindra, A., Laubach, J., Raje, N., Munshi, N., Richardson, P. G., and Anderson, K. (2012) Latest advances and current challenges in the treatment of multiple myeloma. *Nat. Rev. Clin. Oncol. 9*, 135−143.

(2) Anderson, K. C., and Carrasco, R. D. (2012) Pathogenesis of myeloma. *Annu. Rev. Pathol. 6*, 249−274.

(3) Zheng, Y., Cai, Z., Wang, S., Zhang, X., Qian, J., Hong, S., Li, H., Wang, M., Yang, J., and Yi, Q. (2009) Macrophages are an abundant component of myeloma microenvironment and protect myeloma cells from chemotherapy drug-induced apoptosis. *Blood 114*, 3625−3628.

(4) Hideshima, T., Chauhan, D., Schlossman, R., Richardson, P., and Anderson, K. C. (2001) The role of tumor necrosis factor alpha in the pathophysiology of human multiple myeloma: therapeutic applications. *Oncogene 20*, 4519−4527.

(5) Hideshima, T., Podar, K., Chauhan, D., and Anderson, K. C. (2005) Cytokines and signal transduction. *Best Pract. Res., Clin. Haematol. 18*, 509−524.

(6) Chiang, M. Y., and Stadtmauer, E. A. (2004) NF-kappaB, IL-6 and myeloma cell growth: making the connection. *Cancer Biol. Ther. 3*, 1018−1020.

(7) Chauhan, D., Uchiyama, H., Akbarali, Y., Urashima, M., Yamamoto, K., Libermann, T. A., and Anderson, K. C. (1996) Multiple myeloma cell adhesion-induced interleukin-6 expression in bone marrow stromal cells involves activation of NF-kappa B. *Blood 87*, 1104−1112.

(8) Hideshima, T., Chauhan, D., Richardson, P., Mitsiades, C., Mitsiades, N., Hayashi, T., Munshi, N., Dang, L., Castro, A., Palombella, V., Adams, J., and Anderson, K. C. (2002) NF-kappa B as a therapeutic target in multiple myeloma. *J. Biol. Chem. 277*, 16639−16647.

(9) Huston, A., and Roodman, G. D. (2006) Role of the microenvironment in multiple myeloma bone disease. *Future Oncol. 2*, 371−378.

(10) Bommert, K., Bargou, R. C., and Stuhmer, T. (2006) Signalling and survival pathways in multiple myeloma. *Eur. J. Cancer 42*, 1574−1580.

(11) Kisselev, A. F., van der Linden, W. A., and Overkleeft, H. S. (2012) Proteasome inhibitors: an expanding army attacking a unique target. *Chem. Biol. 19*, 99−115.

(12) Stewart, A. K. (2012) Novel therapeutics in multiple myeloma. *Hematology 17* (Suppl 1), S105−108.

(13) Anderson, K. C., Alsina, M., Bensinger, W., Biermann, J. S., Chanan-Khan, A., Cohen, A. D., Devine, S., Djulbegovic, B., Faber, E. A., Jr, Gasparetto, C., Huff, C. A., Kassim, A., Medeiros, B. C., Meredith, R., Raje, N., Schriber, J., Singhal, S., Somlo, G., Stockerl-Goldstein, K., Treon, S. P., Tricot, G., Weber, D. M., Yahalom, J., and Yunus, F. (2012) Multiple myeloma. *J. Natl. Compr. Cancer Network 9*, 1146−1183.

(14) Groll, M., and Potts, B. C. (2011) Proteasome structure, function, and lessons learned from beta-lactone inhibitors. *Curr. Top. Med. Chem. 11*, 2850−2878.

(15) Groll, M., Huber, R., and Moroder, L. (2009) The persisting challenge of selective and specific proteasome inhibition. *J. Pept. Sci. 15*, 58−66.

(16) Groll, M., and Clausen, T. (2003) Molecular shredders: how proteasomes fulfill their role. *Curr. Opin. Struct. Biol. 13*, 665−673.

(17) Groll, M., Ditzel, L., Lowe, J., Stock, D., Bochtler, M., Bartunik, H. D., and Huber, R. (1997) Structure of 20S proteasome from yeast at 2.4 A resolution. *Nature 386*, 463−471.

(18) Groll, M., Heinemeyer, W., Jager, S., Ullrich, T., Bochtler, M., Wolf, D. H., and Huber, R. (1999) The catalytic sites of 20S proteasomes and their role in subunit maturation: a mutational and crystallographic study. *Proc. Natl. Acad. Sci. U.S.A. 96*, 10976−10983.

(19) Kisselev, A. F. (2008) Joining the army of proteasome inhibitors. *Chem. Biol. 15*, 419−421.

(20) Borissenko, L., and Groll, M. (2007) 20S proteasome and its inhibitors: crystallographic knowledge for drug development. *Chem. Rev. 107*, 687−717.

(21) Shah, J. J., and Orlowski, R. Z. (2009) Proteasome inhibitors in the treatment of multiple myeloma. *Leukemia 23*, 1964−1979.

(22) Navon, A., and Ciechanover, A. (2009) The 26 S proteasome: from basic mechanisms to drug targeting. *J. Biol. Chem. 284*, 33713−33718.

(23) Franke, N. E., Niewerth, D., Assaraf, Y. G., van Meerloo, J., Vojtekova, K., van Zantwijk, C. H., Zweegman, S., Chan, E. T., Kirk, C. J., Geerke, D. P., Schimmer, A. D., Kaspers, G. J., Jansen, G., and Cloos, J. (2012) Impaired bortezomib binding to mutant beta5 subunit of the proteasome is the underlying basis for bortezomib resistance in leukemia cells. *Leukemia 26*, 757−768.

(24) Oerlemans, R., Franke, N. E., Assaraf, Y. G., Cloos, J., van Zantwijk, I., Berkers, C. R., Scheffer, G. L., Debipersad, K., Vojtekova, K., Lemos, C., van der Heijden, J. W., Ylstra, B., Peters, G. J., Kaspers, G. L., Dijkmans, B. A., Scheper, R. J., and Jansen, G. (2008) Molecular

basis of bortezomib resistance: proteasome subunit beta5 (PSMB5) gene mutation and overexpression of PSMB5 protein. *Blood 112*, 2489−2499.
(25) Verbrugge, S. E., Assaraf, Y. G., Dijkmans, B. A., Scheffer, G. L., Al, M., den Uyl, D., Oerlemans, R., Chan, E. T., Kirk, C. J., Peters, G. J., van der Heijden, J. W., de Gruijl, T. D., Scheper, R. J., and Jansen, G. (2012) Inactivating PSMB5 mutations and P-glycoprotein (MDR1/ABCB1) mediate resistance to proteasome inhibitors: ex vivo efficacy of (immuno) proteasome inhibitors in mononuclear blood cells from rheumatoid arthritis patients. *J. Pharmacol. Exp. Ther. 341*, 174−182.
(26) de Wilt, L. H., Jansen, G., Assaraf, Y. G., van Meerloo, J., Cloos, J., Schimmer, A. D., Chan, E. T., Kirk, C. J., Peters, G. J., and Kruyt, F. A. (2012) Proteasome-based mechanisms of intrinsic and acquired bortezomib resistance in non-small cell lung cancer. *Biochem. Pharmacol. 83*, 207−217.
(27) Jankowska, E., Gaczynska, M., Osmulski, P., Sikorska, E., Rostankowski, R., Madabhushi, S., Tokmina-Lukaszewska, M., and Kasprzykowski, F. (2010) Potential allosteric modulators of the proteasome activity. *Biopolymers 93*, 481−495.
(28) Wenner, M. (2009) A new kind of drug target. *Sci. Am. 301* (70−74), 76.
(29) Hauske, P., Ottmann, C., Meltzer, M., Ehrmann, M., and Kaiser, M. (2008) Allosteric regulation of proteases. *ChemBioChem 9*, 2920−2928.
(30) Gaczynska, M., and Osmulski, P. A. (2005) Characterization of noncompetitive regulators of proteasome activity. *Methods Enzymol 398*, 425−438.
(31) DeDecker, B. S. (2000) Allosteric drugs: thinking outside the active-site box. *Chem. Biol. 7*, R103−107.
(32) Li, X., Wood, T. E., Sprangers, R., Jansen, G., Franke, N. E., Mao, X., Wang, X., Zhang, Y., Verbrugge, S. E., Adomat, H., Li, Z. H., Trudel, S., Chen, C., Religa, T. L., Jamal, N., Messner, H., Cloos, J., Rose, D. R., Navon, A., Guns, E., Batey, R. A., Kay, L. E., and Schimmer, A. D. (2010) Effect of noncompetitive proteasome inhibition on bortezomib resistance. *J. Natl. Cancer Inst. 102*, 1069−1082.
(33) Groebe, D. R. (2009) In search of negative allosteric modulators of biological targets. *Drug Discovery Today 14*, 41−49.
(34) Anbanandam, A., Albarado, D. C., Tirziu, D. C., Simons, M., and Veeraraghavan, S. (2008) Molecular basis for proline- and arginine-rich peptide inhibition of proteasome. *J. Mol. Biol. 384*, 219−227.
(35) Gaczynska, M., Osmulski, P. A., Gao, Y., Post, M. J., and Simons, M. (2003) Proline- and arginine-rich peptides constitute a novel class of allosteric inhibitors of proteasome activity. *Biochemistry 42*, 8663−8670.
(36) Gao, Y., Lecker, S., Post, M. J., Hietaranta, A. J., Li, J., Volk, R., Li, M., Sato, K., Saluja, A. K., Steer, M. L., Goldberg, A. L., and Simons, M. (2000) Inhibition of ubiquitin-proteasome pathway-mediated I kappa B alpha degradation by a naturally occurring antibacterial peptide. *J. Clin. Invest. 106*, 439−448.
(37) Sprangers, R., Li, X., Mao, X., Rubinstein, J. L., Schimmer, A. D., Kay, L. E., and TROSY-based, N. M. R. (2008) evidence for a novel class of 20S proteasome inhibitors. *Biochemistry 47*, 6727−6734.
(38) Kroll, M., Arenzana-Seisdedos, F., Bachelerie, F., Thomas, D., Friguet, B., and Conconi, M. (1999) The secondary fungal metabolite gliotoxin targets proteolytic activities of the proteasome. *Chem. Biol. 6*, 689−698.
(39) Alexanian, R., Delasalle, K., Wang, M., Thomas, S., and Weber, D. (2012) Curability of multiple myeloma. *Bone Marrow Res. 2012*, 916479.
(40) Lansdell, T. A., O'Reilly, S., Woolliscroft, T., Kahlon, D. K., Hovde, S., McCormick, J. J., Henry, R. W., Cornicelli, J. A., and Tepe, J. J. (2012) Attenuation of collagen-induced arthritis by orally available imidazoline-based NF-kB inhibitors. *Bioorg. Med. Chem. Lett. 22*, 4816−4819.
(41) Kahlon, D. K., Lansdell, T. A., Fisk, J. S., Hupp, C. D., Friebe, T. L., Hovde, S., Jones, A. D., Dyer, R. D., Henry, R. W., and Tepe, J. J. (2009) Nuclear Factor-kappaB mediated inhibition of cytokine production by imidazoline scaffolds. *J. Med. Chem. 52*, 1302−1309.
(42) Baell, J. B., and Holloway, G. A. (2010) New substructure filters for removal of pan assay interference compounds (PAINS) from screening libraries and for their exclusion in bioassays. *J. Med. Chem. 53*, 2719−2740.
(43) Dominquez, A., Fernandez, A., Gonzalez, N., Iglesias, E., and Montenegro, L. (1997) Determination of critical micelle concentration of some surfactants by three techniques. *J. Chem. Educ. 74*, 1227−1231.
(44) Thompson, S. J., Loftus, L. T., Ashley, M. D., and Meller, R. (2008) Ubiquitin-proteasome system as a modulator of cell fate. *Curr. Opin. Pharmacol. 8*, 90−95.
(45) Baud, V., and Karin, M. (2009) Is NF-kappaB a good target for cancer therapy? Hopes and pitfalls. *Nat. Rev. Drug Discovery 8*, 33−40.
(46) Chen, Z. J. (2005) Ubiquitin signalling in the NF-kappaB pathway. *Nat. Cell Biol. 7*, 758−765.
(47) Sharma, V., Lansdell, T. A., Peddibhotla, S., and Tepe, J. J. (2004) Sensitization of tumor cells towards chemotherapy: Enhancing the efficacy of camptothecin by novel imidazolines. *Chem. Biol. 11*, 1689−1699.
(48) Segel, I. H. (1975) *Enzyme Kinetics*, John Wiley & Sons, Inc, New York.
(49) Borodovsky, A., Ovaa, H., Meester, W. J., Venanzi, E. S., Bogyo, M. S., Hekking, B. G., Ploegh, H. L., Kessler, B. M., and Overkleeft, H. S. (2005) Small-molecule inhibitors and probes for ubiquitin- and ubiquitin-like-specific proteases. *ChemBioChem 6*, 287−291.
(50) Richards, T., and Weber, D. (2010) Advances in treatment for relapses and refractory multiple myeloma. *Med. Oncol. 27* (Suppl 1), S25−42.
(51) Rossia, M., Di Martino, M. T., Morelli, E., Leotta, M., Rizzo, A., Grimaldi, A., Misso, G., and Caraglia, M. (2012) Molecular targets for the treatment of multiple myeloma. *Curr. Cancer Drug Targets 12*, 757−767.
(52) Heaney, N. B., Pellicano, F., Zhang, B., Crawford, L., Chu, S., Kazmi, S. M., Allan, E. K., Jorgensen, H. G., Irvine, A. E., Bhatia, R., and Holyoake, T. L. (2010) Bortezomib induces apoptosis in primitive chronic myeloid leukemia cells including LTC-IC and NOD/SCID repopulating cells. *Blood 115*, 2241−2250.
(53) Meng, L., Mohan, R., Kwok, B. H., Elofsson, M., Sin, N., and Crews, C. M. (1999) Epoxomicin, a potent and selective proteasome inhibitor, exhibits in vivo antiinflammatory activity. *Proc. Natl. Acad. Sci. U.S.A. 96*, 10403−10408.
(54) Uluckan, O., Becker, S. N., Deng, H., Zou, W., Prior, J. L., Piwnica-Worms, D., Frazier, W. A., and Weilbaecher, K. N. (2009) CD47 regulates bone mass and tumor metastasis to bone. *Cancer Res. 69*, 3196−3204.